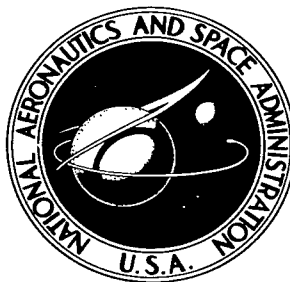


NASA TECHNICAL NOTE



NASA TN D-4027

c.1

LOAN COPY: RETURN TO
AFWL (WJL-2)
KIRTLAND AFB, N MEX



NASA TN D-4027

A LINEARIZED ERROR ANALYSIS OF ONBOARD PRIMARY NAVIGATION SYSTEMS FOR THE APOLLO LUNAR MODULE

*by Jerrold H. Suddath, Robert H. Kidd III,
and Arnold G. Reinhold*

*Manned Spacecraft Center
Houston, Texas*



A LINEARIZED ERROR ANALYSIS OF ONBOARD PRIMARY
NAVIGATION SYSTEMS FOR THE APOLLO
LUNAR MODULE

By Jerrold H. Suddath, Robert H. Kidd III,
and Arnold G. Reinhold

Manned Spacecraft Center
Houston, Texas

NATIONAL AERONAUTICS AND SPACE ADMINISTRATION

For sale by the Clearinghouse for Federal Scientific and Technical Information
Springfield, Virginia 22151 - CFSTI price \$3.00

ABSTRACT

A study has been made to determine the accuracies which could be expected from onboard primary navigation systems for the lunar module following the concentric flight plan. Emphasis was placed on comparing a rendezvous radar with an optical tracker as a source of navigational information. The comparison was drawn from linearized error analyses of the navigation systems as they would function in various phases of the concentric flight plan. The results of the investigation indicate that there is little difference between rendezvous radar and optical tracker performance in the primary navigation system in terms of navigation accuracy. Furthermore, for either sensor, the effect of reduced accuracy and the effect of varying the measurement sampling period on navigation accuracy are of little significance.

**A LINEARIZED ERROR ANALYSIS OF ONBOARD PRIMARY
NAVIGATION SYSTEMS FOR THE APOLLO
LUNAR MODULE**

**By Jerrold H. Suddath, Robert H. Kidd III,
and Arnold G. Reinhold
Manned Spacecraft Center**

SUMMARY

A study has been made to determine the accuracies which could be expected from onboard primary navigation systems for the lunar module following the concentric flight plan. Emphasis was placed on comparing a rendezvous radar with an optical tracker as a source of navigational information. The comparison was drawn from linearized error analyses of the navigation systems as they would function in various phases of the concentric flight plan. The results of the investigation indicate that there is little difference between rendezvous radar and optical tracker performance in the primary navigation system in terms of navigation accuracy. Furthermore, for either sensor, the effect of reduced accuracy and the effect of varying the measurement sampling period on navigation accuracy are of little significance.

INTRODUCTION

The purpose of this study was to compare a rendezvous radar with an optical tracker as a source of navigational information in an onboard primary navigation system for the Apollo lunar module (LM). The comparison was drawn from error analyses of one system with an optical tracker and another system with a rendezvous radar. Included in this comparison are the effects of sun and moon interference on the sensors, the inertial platform alignment accuracies of the two systems, the command and service module (CSM) ephemeris uncertainties, and the navigation sensor reference misalignment.

The error analyses were performed by using a digital computer to calculate the covariance matrix for the errors of a navigation system (using either the radar or tracker) as a function of time along the trajectories of interest. It was assumed that the navigation system would estimate the state (position and velocity) of the LM measured relative to the CSM and that the estimation would be done with a Kalman filter (ref. 1). Results are presented in the form of time histories of root mean square (rms) relative position and velocity estimation uncertainties for the trajectories considered.

SYMBOLS

B	Jacobian matrix for measurement
\bar{e}_k	error in the CSM state estimate at time t_k
F	matrix defined in equation (4)
f*	matrix defined in equation (5)
g*	matrix defined in equation (6)
I	identity matrix
K	gain matrix
M_k	covariance matrix of the relative state estimation error before an update
\bar{m}	measurement vector
m_i	ith component of \bar{m}
P_k	covariance matrix of \bar{e}_k
R	covariance matrix of measurement noise
\bar{R}_C	radius vector of CSM
\bar{R}_L	radius vector of LM
r_C	$ \bar{R}_C $
r_L	$ \bar{R}_L $
S_k	covariance matrix of \bar{u}_k
T	matrix defined in equation (9)
t	time
t_k	time after k program steps
\bar{u}_k	error in measuring velocity correction at time t_k ; null if no correction is made

\bar{u}_{SL}	unit vector in direction of sun
Z_k	cross correlation matrix of \bar{e}_k and $\bar{\epsilon}_k$
\bar{z}	measurement vector plus noise
α^*	matrix defined in equation (4)
β^*	matrix defined in equation (5)
Γ	additional transition matrix for relative deviations
γ^*	matrix defined in equation (6)
ΔV	change in velocity vector
$\bar{\epsilon}_k$	error in the estimate of the relative state at time t_k
ζ	angle between the line of sight to the sun and the line of sight to the CSM, degrees
ζ^*	critical angle ζ , degrees
Θ	fundamental matrix for relative deviations
θ_{ij}	partition of Θ defined in equation (9)
μ	gravitational constant for the moon
$\bar{\nu}$	measurement noise vector
π_k	covariance matrix of $\bar{\epsilon}_k$
$\bar{\rho}$	relative displacement vector, $\bar{R}_L - \bar{R}_C$
ρ_j	jth component of $\bar{\rho}$
σ	standard deviation
Φ	transition matrix for CSM deviations

Operators:

$E(\cdot)$	expected value of (\cdot)	$\ \cdot \ $	Euclidean norm
$(\cdot)^T$	matrix transpose	$(\cdot\cdot)$	second derivative of variable

SCOPE OF THE STUDY

To compare a rendezvous radar with an inertially referenced, optical line-of-sight tracker as a source of navigational information for the LM, it was necessary to consider the salient characteristics of the overall LM mission. In this study, the LM mission was taken to be that of following the concentric flight plan (fig. 1). The nominal sequence of events on this flight plan was taken to be the following:

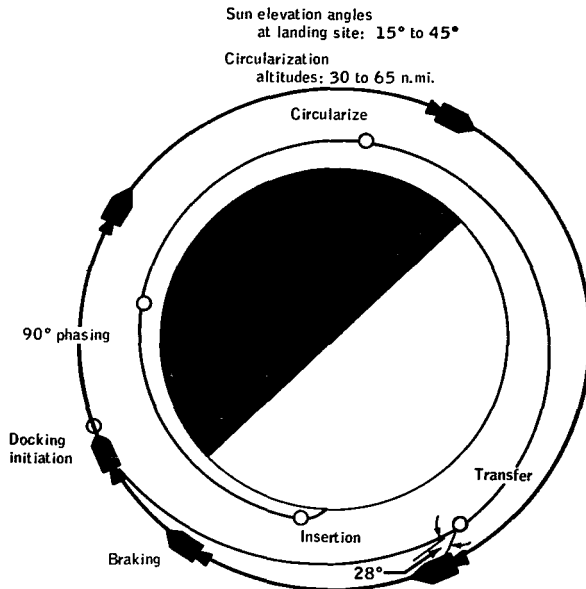


Figure 1. - Concentric flight plan.

- (1) LM separation from CSM
- (2) Hohmann descent
- (3) Powered descent
- (4) Landing
- (5) Nominal launch
- (6) 90° burn to adjust apocynthion
- (7) Circularization
- (8) Transfer maneuver
- (9) Terminal rendezvous

In addition to the nominal sequence of events, there were the following contingencies to be examined:

- (1) Abort 12 minutes after LM separation; 70° direct transfer to rendezvous
- (2) Abort 35 minutes after LM separation; 140° direct transfer to rendezvous
- (3) Abort from start of powered descent
- (4) Abort from hover
- (5) Late launch

The necessity of having to consider all these phases of the mission arose because there are physical limitations on both sensors which restrict their ability to track. For example, the optical tracker cannot track if the angle between the lines of sight (LOS) to the sun and to the CSM is less than some critical value which is shown in figure 2 as a function of relative range. Also, the tracker cannot track the CSM against a fully illuminated lunar background at ranges greater than 40 nautical miles. Moreover, neither the tracker nor the radar can track at ranges greater than 400 nautical miles. Thus, every phase of the mission had to be examined to see if these limitations created any major problem areas.

METHOD OF ANALYSIS

Angle bias (1σ) = 0.2 mr
Random angle (3σ) = 0.45 mr

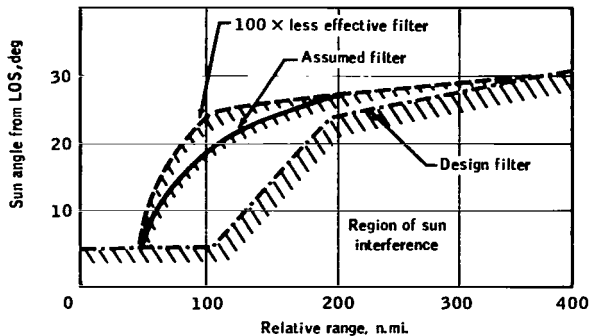


Figure 2. - Optical tracker error model and sun angle constraint.

The error analyses were performed by using a digital computer to calculate the covariance matrix for the errors of a navigation system (using either radar or tracker) as a function of time along the trajectories of interest. The computer program used is described in the appendix.

The rms relative position uncertainty was obtained by taking the square root of the sum of the first three diagonal elements of the covariance matrix. Similarly, the rms relative velocity uncertainty was obtained by taking the square root of the sum of the second three diagonal terms of the covariance matrix.

Navigational measurements were simulated only in the sense of computing their effects on the statistics of the estimation process.

To do this type of error analysis, certain a priori statistics must be given. Also, statistical error models are necessary for the radar, tracker, accelerometers, coupling data unit, and inertial platform and sensor reference misalignments with respect to the inertial platform. The error models used in this study are discussed in the next section.

ERROR MODELS

Optical Tracker

In using the model for the optical tracker, it was assumed that the tracker would measure the azimuth and elevation angles of the CSM relative to an inertial coordinate system (the inertial platform). The sun interference constraint is plotted in figure 2. Other pertinent data are

Bias (1σ) = 0.2 milliradian (mr)

Noise (1σ) = 0.15 mr

For the tracker, specification data indicated that sensor reference misalignment errors were negligible.

Rendezvous Radar

In using the model for the radar, it was assumed that the radar would measure either relative range or relative range rate and shaft and trunnion angles (defining the line of sight to the CSM) relative to the sensor reference. Pertinent data for the radar are listed below.

Range bias (3σ) = 1500 feet

Range noise (3σ) = greater of 0.25 percent or 300 feet

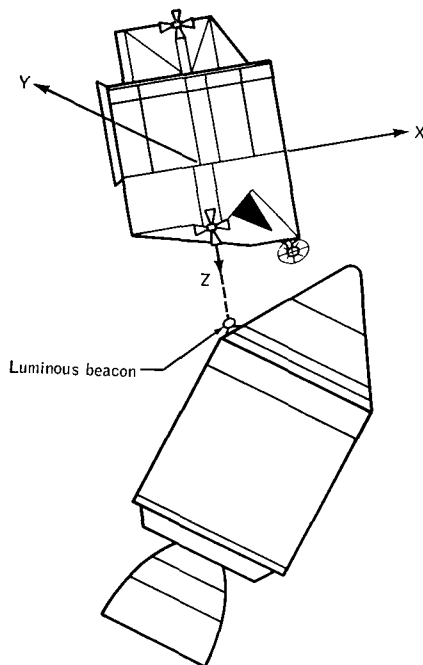
Range-rate bias (3σ) = 3 ft/sec

Range-rate noise (3σ) = greater of 0.25 percent or 1 ft/sec

Angle bias (3σ) = 7 mr (including sensor reference misalignment)

Angle noise (3σ) = 2 mr for range < 200 nautical miles linearly increasing to 4 mr at 400 nautical miles

For the rendezvous radar, the sensor reference misalignment errors (specification values) are significant to the point where vehicle attitude must be known to represent the errors in a measurement. This being the case, vehicle attitude profiles had to be assumed in the simulations of the radar. The nominal attitude profile used in all radar simulations is described as follows:



(1) No roll or yaw; LM X-Z plane always coincident with orbital plane (fig. 3)

(2) Pitch vehicle so as to maintain LM Z-axis along line of sight from LM to CSM

The reasons for selecting this attitude profile are the following:

(1) With the vehicle Z-axis along the line of sight, the radar is always bore-sighted down the Z-axis. This attitude tends to minimize the radar boresight drift error, since it is a function of the shaft and trunnion angles which, in this case, are nominally zero.

Figure 3. - LM attitude profile.

(2) Since the normal field of view for the astronauts is in the direction of the LM Z-axis, this attitude profile keeps the CSM in their field of view at all times.

(3) This attitude profile also simplifies the mechanization of the onboard navigation system.

Inertial Platform Errors

When a ΔV maneuver is made, the errors in the estimate of the applied ΔV increase the uncertainties in the estimate of the vehicle velocity. Since the inertial platform measures the applied ΔV , the error estimating the applied ΔV comes from the inertial platform errors. Therefore, after a ΔV maneuver, the covariance matrix for the error in the navigational estimate must be updated according to the error model for the inertial platform. The data used for the inertial platform errors (specification values) are given below.

$$\text{Accelerometer bias (1 } \sigma) = 0.00656 \text{ ft/sec}^2$$

$$\text{Accelerometer scale factor (1 } \sigma) = 100 \text{ parts per million}$$

$$\text{Gyro drift (1 } \sigma) = 0.5 \text{ mr/hr}$$

$$\text{Platform alinement: Optical Tracker (1 } \sigma) = 0.2 \text{ mr}$$

$$\text{Platform alinement: Rendezvous Radar (1 } \sigma) = 1 \text{ mr}$$

The inertial platform was assumed to be realigned within 15 minutes of each ΔV maneuver. This essentially eliminates the effect of gyro drift on the measurement of the ΔV maneuver compared with the effect of alinement inaccuracy. An alinement optical telescope is used to align the platform in the rendezvous radar system.

RESULTS AND DISCUSSION

Various trajectories associated with the concentric flight plan were simulated by using the error models presented in the previous sections and the computer program described in the appendix. The three basic cases considered for each trajectory were:

(1) Navigational information provided by optical tracker measuring azimuth and elevation angles

(2) Navigational information provided by rendezvous radar measuring shaft and trunnion angles and range

(3) Navigational information provided by rendezvous radar measuring shaft and trunnion angles and range rate

The results of the simulations are discussed in the following sections.

Nominal Launch

The geometry of the nominal launch trajectory is represented in figure 1. The trajectory consists of the following sequence of events:

- (1) Powered ascent from launch site (taken to be 0° long., 0° lat.) to ascent injection
- (2) Coast through approximately 90° central angle
- (3) At approximately 90° , a ΔV maneuver is made to adjust the altitude and longitude of apocynthion
- (4) Circularization of the orbit at apocynthion and coast to transfer
- (5) At the transfer point, a ΔV maneuver is made to put the LM on a 140° direct transfer to rendezvous

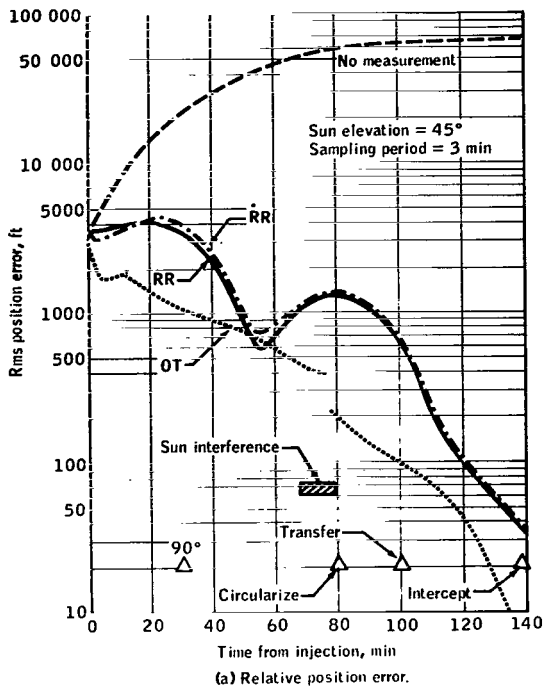
The simulation of this phase was initiated at ascent injection. Navigational measurements were assumed to be made every 3 minutes if the constraints on the sensors were satisfied.

Results of the simulations are shown in figure 4. Figure 4(a) is a semilog plot of the rms relative position uncertainties in feet versus time after ascent injection in minutes.

The curve at the top of the figure is for the case where no measurements are made throughout the trajectory. In this case, the rms relative position uncertainty begins at about 3700 feet and simply grows to about 68 000 feet at the time of rendezvous.

The curve at the bottom of the figure is for the case where the optical tracker was used to make measurements. The initial uncertainty for this case is about 400 feet less than for the other cases plotted on the figure, which results because prior to launch the platform is realigned, and alinement with the optical tracker system is more accurate than alinement with the radar system. Therefore, when the alinement errors are propagated through the powered ascent, the tracker system has smaller injection errors than the radar system.

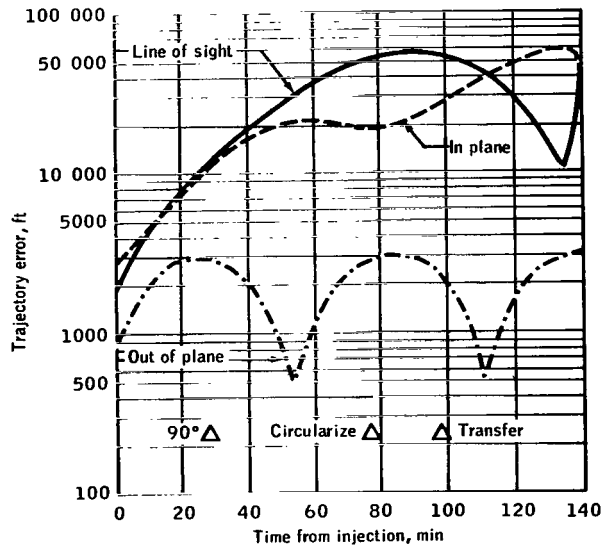
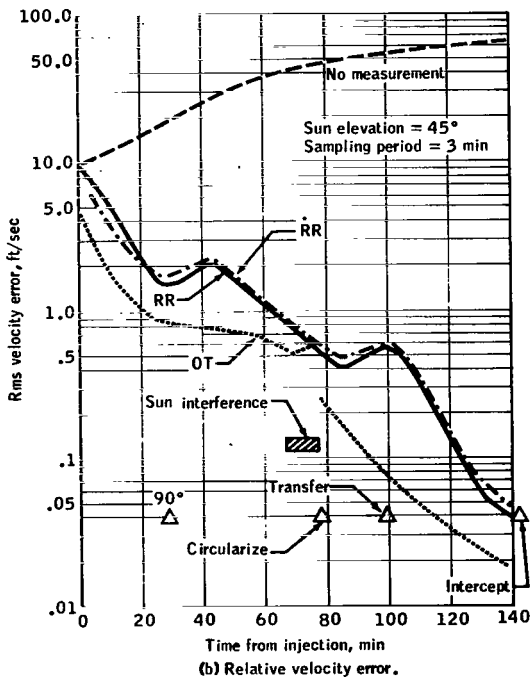
The optical tracker experiences sun interference, which is indicated in figure 4(a) as occurring at 67 minutes and lasting until 78 minutes after injection. This trajectory was computed assuming that the sun elevation angle (relative to the lunar local horizontal) at the landing point was 45° , and the lunar stay time was 36 hours. However, other trajectories were computed with the elevation angle being varied upward from an elevation of 15° , and no significant difference was noted in the performance of the tracker system. Therefore, this case was presented as being typical of any sun elevation angle currently being considered for the concentric flight plan, and it was concluded that sun interference with the optical tracker is not a problem on the nominal launch.



The two curves in the middle of figure 4(a) are for the two cases where the rendezvous radar was the sensor. In both cases, shaft and trunnion angles were measured so that the cases differ only in that range was the third measurable in one case, whereas range rate was the third measurable in the other case. The two types of radar provided very little difference in the navigational accuracy.

Figure 4(b) is a semilog plot of the rms relative velocity uncertainties in feet per second versus time after injection in minutes. The description of this plot is virtually the same as the preceding description of figure 4(a).

The "lumps" on the radar curves are caused by out-of-plane errors and are easily seen by examination of figure 4(c) which is a plot of the components of the relative position uncertainties along the line of sight, out of plane, and in the orbital plane normal to the



(c) Trajectory error with no measurements - nominal launch.

Figure 4. - Relative position and velocity error for nominal launch: range radar (RR), range rate radar (RR), optical tracker (OT).

line of sight. Although the plot is for the case where no measurements are made, the periodic character of the out-of-plane error is very evident in the radar errors plotted in figure 4(a).

In the navigation system of this study, the relatively large radar out-of-plane errors were due to a misalignment bias. If necessary, the error could be reduced substantially by simply estimating this bias, which would essentially eliminate any difference between the radar and tracker accuracies, but would impose some additional computational requirements on the radar system. Overall comparison of the curves on figures 4(a) and 4(b) shows that there is little difference in navigation accuracy using either the optical tracker or the rendezvous radar in the primary navigation mode.

Late Launch

The geometry and sequence of events for the late launch trajectory are basically the same as for the nominal launch trajectory. The only substantial difference is the position of the CSM at launch. Figure 5 is a semilog plot of the rms relative position uncertainty in feet versus time after injection in minutes. The description of this plot is similar to the description of figure 4(a).

During the first 21 minutes of the late launch trajectory, neither the optical tracker nor the radar can make measurements, because the relative range during this period is greater than 400 nautical miles. Once again the optical tracker experienced sun interference, but it was found that interference is not a problem on the late launch.

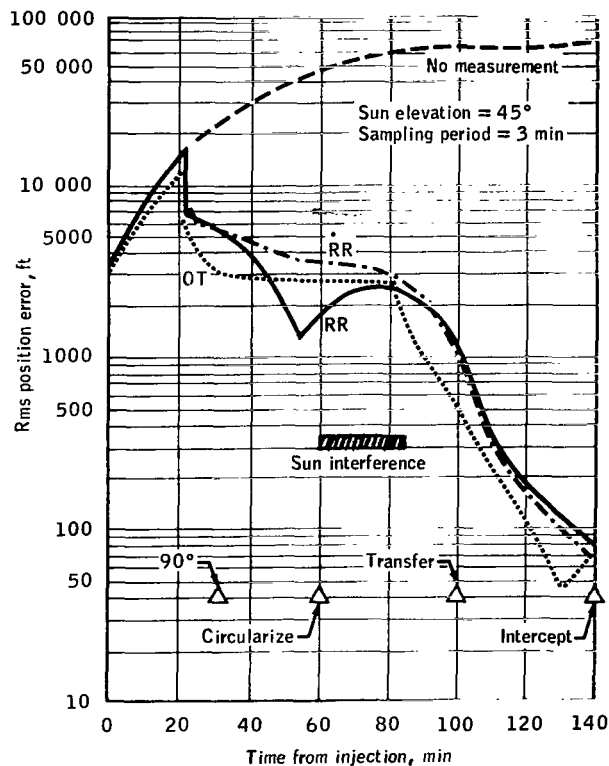


Figure 5. - Relative position error for late launch: range radar (RR), range rate radar (RR), optical tracker (OT).

Abort Trajectory Results

The geometry of the abort from start of powered descent is shown in figure 6. A semilog plot of the relative position error for an abort 12 minutes after LM-CSM separation, which is a direct transfer through 70° , is shown in figure 7.

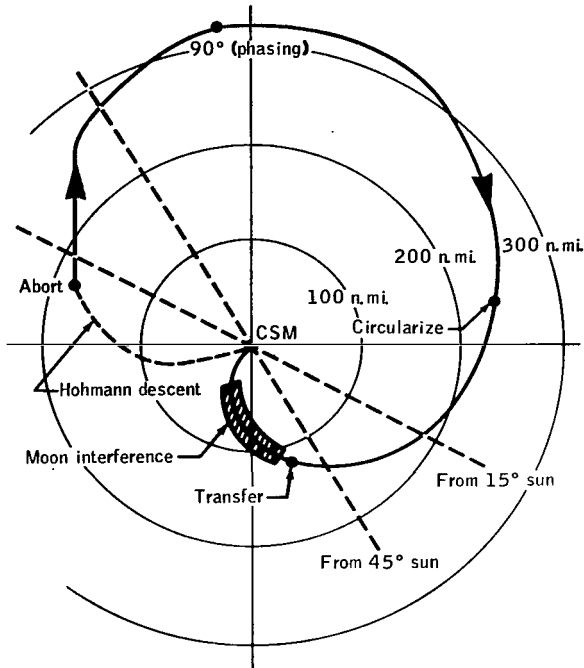


Figure 6. - LM-CSM relative inertial position for abort from start of powered descent.

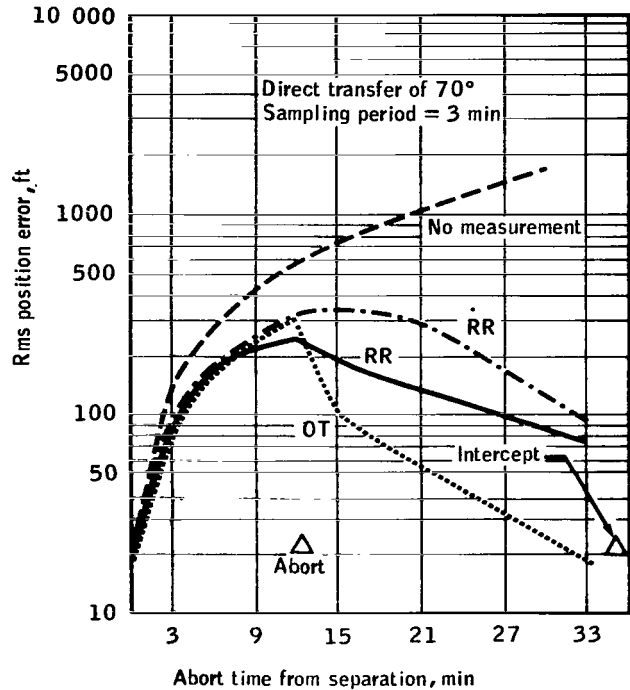


Figure 7. - Relative position error for an abort 12 minutes after LM-CSM separation: range radar (RR), range rate radar (RR), optical tracker (OT).

The relative position error for an abort 35 minutes after LM-CSM separation is shown in figure 8 using a direct transfer through 140° . This plot is virtually the same as the other abort, with no sun interference on the tracker for this and the above abort case for a sun elevation at the landing site corresponding to 15° to 45° .

Figure 9 shows relative position error for an abort from the start of powered descent, with the only difference about this plot being the moon interference toward the end of the trajectory. The error in the optical tracker increases slowly during the period of moon interference, but once track is reestablished, the error comes back down. Therefore, moon interference with the tracker does not appear to be a problem.

The relatively large buildup of errors during the first portion of the trajectories is caused by the optical tracker being hampered by the existence of a low line-of-sight rate during the first part of the trajectory. Whenever this is the case, the tracker

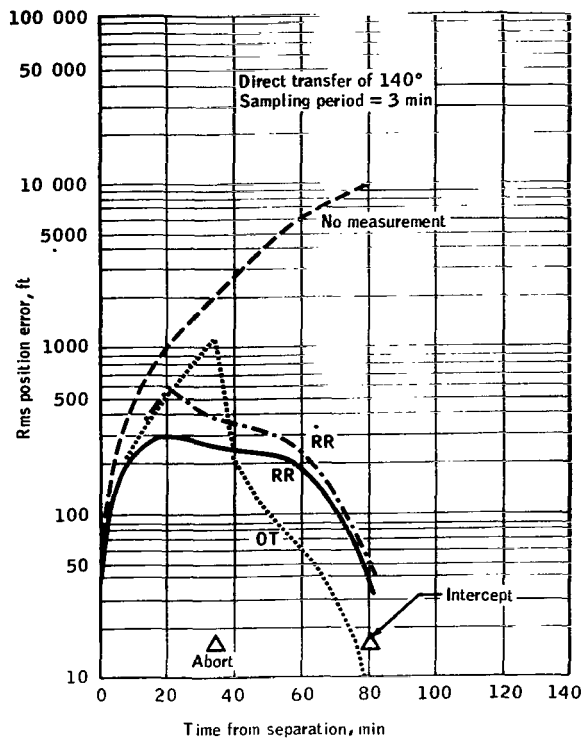


Figure 8. - Relative position error for an abort 35 minutes after LM-CSM separation: range radar (RR), range rate radar (RR), optical tracker (OT).

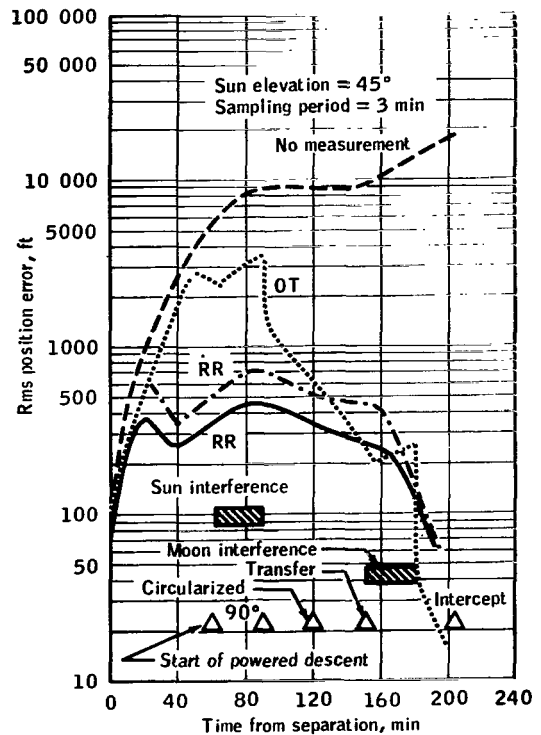


Figure 9. - Relative position error for abort from start of powered descent: range radar (RR), range rate radar (RR), optical tracker (OT).

does not provide much information, and the error tends to grow. The radar error grows at the beginning of the trajectory because of the rather large initial bias in the range. Even though the bias is being estimated, a certain amount of information coming in is required to estimate this bias. Therefore, during the first part of the trajectory, most of the information is going into the estimation of bias and very little into the estimation of the state. Once the bias estimate becomes fairly good, the radar errors tend to decrease until the point is reached in the trajectory where relative range becomes quite large. Since the noise in the radar range measurement is a function of the range, the noise is increasing and, therefore, causing errors to increase during the middle portion of the trajectory.

Little difference was noted between the navigation accuracies obtained with radar and optical tracker for the abort trajectories considered, which is consistent with the statement made earlier for the nominal launch trajectory.

Effect of the Sampling Period

The effect of the sampling period on relative position error for the optical tracker for the nominal launch trajectory is shown in figure 10. The solid curve shows the error if one measurement is made every 3 minutes, and the dashed curve shows the error if there is only one measurement made every 9 minutes. After a measurement is made on the 9-minute, sampling-period case, the error is very close to the 3-minute sampling-period curve. When this fact is remembered and the estimate only noted immediately after making a measurement, then increasing the sample period without significantly degrading the accuracy of the system can be concluded.

The effect of the sampling period on relative position error for the range radar shown in figure 11 is very similar to the effect of the sampling period on the optical tracker (compare fig. 11 with fig. 10), and the same conclusions apply.

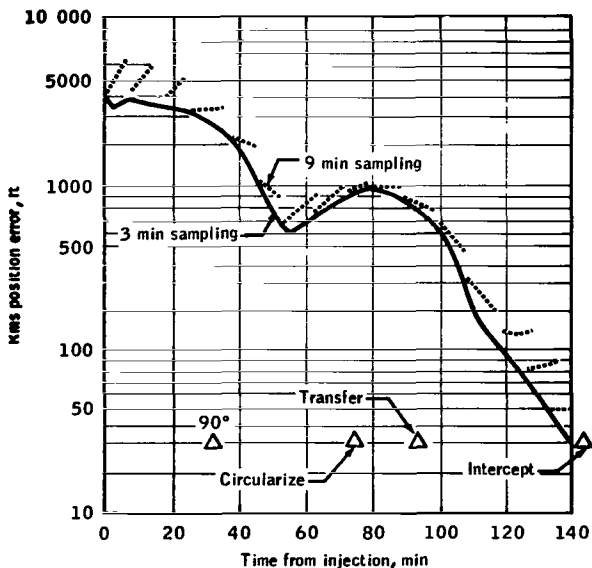
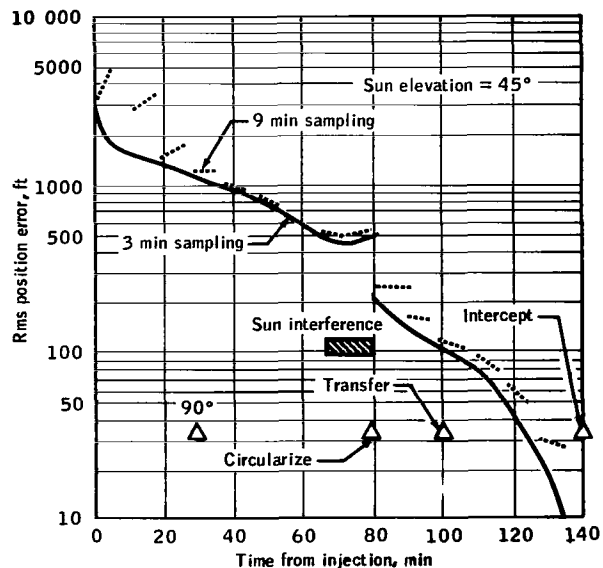


Figure 10. - Effect of sampling period on optical tracker relative position error for nominal launch. Sampling period equals time between measurements.

Figure 11. - Effect of sampling period on range radar relative position error for nominal launch. Sampling period equals time between measurements.

Effect of Sensor Accuracy

The effect of optical tracker accuracy on the relative position errors on the nominal launch trajectory is shown in figure 12. The dashed curve is the performance obtained if the tracker has the specification value for the noise. The solid curve is the error if the errors were three times the specification values. While there is some degradation in the performance of the system with the errors being increased by the factor of three, the degradation does not appear significant.

The effect of range radar accuracy on relative position errors for nominal launch is shown in figure 13. The dashed curve is for the radar with the specification values. The solid curve is for three times the specification values. The dotted curve is for specification noise, but the angle bias is reduced to 1 milliradian. Once again, some degradation occurs when the noise and bias are three times the specification values; but since the errors are probably significant only at the end of the trajectory, the degradation does not seem to be very serious.

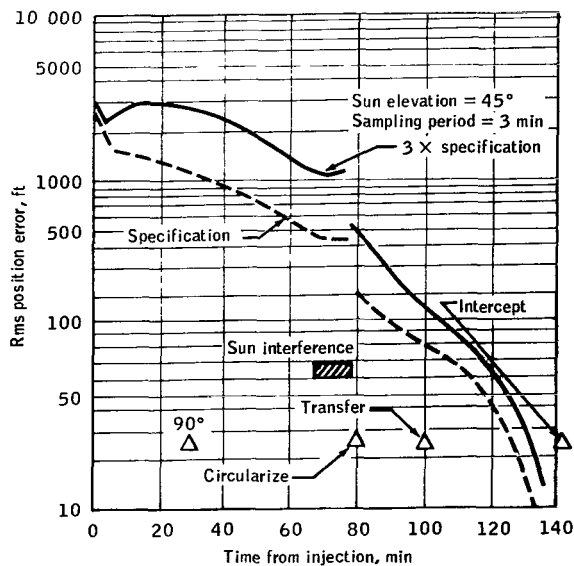


Figure 12. - Effect of optical tracker accuracy on relative position error for nominal launch.

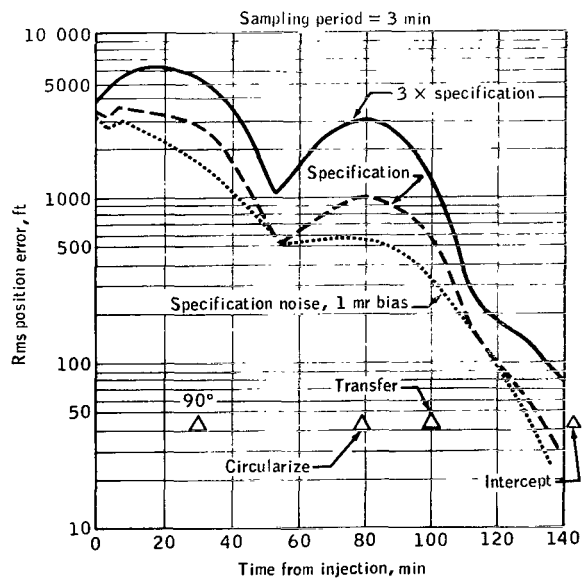


Figure 13. - Effect of range radar accuracy on relative position error for nominal launch.

CONCLUDING REMARKS

A study was made to determine the accuracies which could be expected from on-board primary navigation systems for the lunar module following the concentric flight plan. Emphasis was placed on comparing a rendezvous radar with an optical tracker as a source of navigational information. The comparison was drawn from error analyses of the navigation systems as they functioned in various phases of the concentric flight plan. The results of the investigation indicate little difference in terms of navigation accuracy between rendezvous radar and optical tracker performance for specification error models in the primary navigation system. Sun interference has little effect on the accuracy of the primary system with the optical tracker. Furthermore, the effects of measurement sampling period and degraded systems have little significance.

Manned Spacecraft Center
National Aeronautics and Space Administration
Houston, Texas, January 20, 1967
914-30-50-01-72

APPENDIX

The purpose of this appendix is to describe a computer program which provides the capability to perform error analyses of LM-CSM rendezvous trajectories. Particular attention has been given to the simulation of the concentric flight plan, but the basic program has the capability of simulating virtually any type of rendezvous trajectory with only moderate alterations.

For convenience, this appendix is divided into two main sections. The first section is a verbal description of what the program does in terms of what is computed and how it is computed. The second section presents the appropriate equations which correspond to the description given in the first section.

Description of the Program

Dynamics. - The CSM is assumed to be in an orbit about the moon. The equations of motion for the CSM are written relative to an inertial coordinate system centered in the moon, which is assumed to have an inverse square, central force field. This representation of the potential of the moon is adequate for this type of investigation.

The LM is assumed to be on a trajectory which would lead to rendezvous with the CSM. The motion of the LM is described by its position and velocity measured relative to that of the CSM.

An LM guidance maneuver is represented by simply adding a ΔV to the LM velocity vector.

Navigation system. - The navigation system is simulated by assuming that measurements would be processed by a Kalman filter. The use of this filter entails linearization about nominal trajectories, white Gaussian noise representation of random input variables, and a certain amount of given, a priori statistics.

The program will compute the covariance matrix of the error in the estimate of the deviations from the nominal relative state of the LM. The corresponding covariance matrix for the CSM is also computed.

Measurements. - Either optical sightings or radar measurements can be simulated. In the case of optical sightings, a measurement consists of the simultaneous reading of two angles plus bias and random errors. Radar measurements consist of the simultaneous reading of two angles, range or range rate, plus bias and random errors.

The angle measurements programed for the optical tracker are azimuth and elevation, as opposed to two gimbal angles for the radar shaft and trunnion. In addition, the angular bias errors are assumed to be initially independent, and the noise errors perpetually independent. This situation is only approximately correct because of the actual angles measured, the inertial platform misalignment, and the sensor reference misalignment. The drift of the gyros is programed to affect the two biases independently, and drifts between integration steps are assumed to be independent. Additionally,

before a ΔV maneuver, the inertial platform is realigned, and the bias estimation is reinitialized.

Measurements are simulated only in the sense of computing their effects on the statistics of the estimation process.

Measurement constraint. - In simulating measurements made by an optical tracker, it should be noted that the tracker cannot track if the angle between the lines of sight to the sun and to the vehicle is less than some critical value. Moreover, this critical angle is a function of the range between the vehicles. This effect is simulated in the program by prohibiting optical measurements when a constraint is not satisfied.

Equations for the Program

Dynamic equations. - The equations of motion for the CSM are given by

$$\ddot{\bar{\mathbf{R}}_C} = -\frac{\mu}{r_C^3} \bar{\mathbf{R}}_C \quad (1)$$

where

$\bar{\mathbf{R}}_C$ = radius vector of CSM

$$r_C = \|\bar{\mathbf{R}}_C\|$$

μ = gravitational constant for moon

Let $\bar{\mathbf{R}}_L$ denote the radius vector of LM and define the relative vector

$$\bar{\rho} = \bar{\mathbf{R}}_L - \bar{\mathbf{R}}_C \quad (2)$$

The differential equation for $\bar{\rho}$ is

$$\ddot{\bar{\rho}} = -\frac{\mu}{r_L^3} \left\{ \bar{\rho} + \left[1 - \left(\frac{r_L}{r_C} \right)^3 \right] \bar{\mathbf{R}}_C \right\} \quad (3)$$

where

$$r_L = \left\| \bar{R}_L \right\| = \left\| \bar{\rho} + \bar{R}_C \right\|$$

Nominal trajectories (solutions of equations (1) and (3) for $\bar{R}_C(t)$ and $\bar{\rho}(t)$) are needed to compute coefficients in the matrix differential equations given in the next section.

Transition matrices. - The transition matrix for CSM deviations is denoted by Φ and computed from

$$\frac{d}{dt} \Phi(t, t_0) = F(t) \Phi(t, t_0), \quad \Phi(t_0, t_0) = I \quad (4)$$

where

$$F(t) = \begin{bmatrix} 0 & I \\ \alpha^*(t) & 0 \end{bmatrix}$$

and

$$\alpha^*(t) = - \frac{\mu}{r_C} \frac{3}{2} \left[I - \frac{3}{r_C} \bar{R}_C(t) \bar{R}_C^T(t) \right]$$

where I denotes the identity matrix. The concepts of transition and fundamental matrices are treated in reference 2. The fundamental matrix for relative deviations is denoted by Θ and computed from

$$\frac{d}{dt} \Theta(t, t_0) = f^*(t) \Theta(t, t_0), \quad \Theta(t_0, t_0) = I \quad (5)$$

where

$$f^*(t) = \begin{bmatrix} 0 & I \\ \beta^*(t) & 0 \end{bmatrix}$$

and

$$\beta^*(t) = -\frac{\mu}{r_L^3} \left[I - \frac{3}{r_L^2} (\bar{\rho} + \bar{R}_C)(\bar{\rho} + \bar{R}_C)^T \right]$$

Since the relative state is a function of the CSM state (see equation (3)), the additional transition matrix for relative deviations is denoted by Γ and computed from

$$\frac{d}{dt} \Gamma(t, t_0) = f^*(t) \Gamma(t, t_0) + g^*(t) \Phi(t, t_0) \quad (6)$$

where

$$\Gamma(t_0, t_0) = 0$$

and

$$g^*(t) = \begin{bmatrix} \gamma^*(t) & 0 \\ 0 & 0 \end{bmatrix}$$

$$\gamma^*(t) = \frac{\mu}{r_L^3} \left[\left(\frac{r_L^3}{r_C^3} - 1 \right) I + \frac{3}{r_L^2} (\bar{\rho} + \bar{R}_C)(\bar{\rho} + \bar{R}_C)^T - \frac{3r_L^3}{r_C^5} \bar{R}_C \bar{R}_C^T \right]$$

CSM Errors

It is assumed that the estimate of the CSM state is not updated during the flight. Therefore, if the error in the estimate at time t_k is denoted by \bar{e}_k , and if P_k is defined as

$$P_k = E(\bar{e}_k \bar{e}_k^T)$$

then

$$P_{k+1} = \Phi(t_{k+1}, t_k) P_k \Phi^T(t_{k+1}, t_k) \quad (7)$$

where it is assumed that P_0 will be given. If the estimate of the CSM state is the nominal trajectory, then P_k is also the covariance matrix of the CSM dispersions, and the dispersions are the negative of the errors.

Relative state estimation errors. - The propagation of relative state estimation errors is done in the following way.

Noting that

$$\bar{\epsilon}_{k+1} = \Theta \bar{\epsilon}_k + \Gamma \bar{e}_k + T \bar{u}_k$$

the covariance matrix of the relative state estimation error before an update is

$$M_{k+1} = \Theta \pi_k \Theta^T + T S_k T^T + \Gamma P_k \Gamma^T + \Theta Z_k \Gamma^T + \Gamma Z_k^T \Theta^T \quad (8)$$

where the arguments of Θ , Γ , and T are (t_{k+1}, t_k) , and

$$\pi_k = E(\bar{\epsilon}_k \bar{\epsilon}_k^T)$$

$$Z_k = E(\bar{\epsilon}_k \bar{e}_k^T)$$

$$S_k = E(\bar{u}_k \bar{u}_k^T)$$

\bar{u}_k = error in measuring a ΔV correction at time t_k ;
null if no correction is made

where

$\bar{\epsilon}_k$ = error in estimating relative state at time t_k

If Θ is partitioned thus,

$$\Theta = \begin{bmatrix} \theta_{11} & \theta_{12} \\ \theta_{21} & \theta_{22} \end{bmatrix} \quad (9)$$

then T is defined by

$$T = \begin{bmatrix} \theta_{12} \\ \theta_{22} \end{bmatrix}$$

Second, compute the gain matrix K from

$$K = MB^T(BMB^T + R)^{-1} \quad (10)$$

where all matrices in equation (10) are understood to have subscript $k+1$. The covariance matrix for measurement noise is R , and the Jacobian matrix of the measurement is B . Thus, if \bar{z} denotes the vector valued measurement given by

$$\bar{z} = \bar{m}(\bar{\rho}) + \bar{\nu}$$

then

$$R = E\left(\bar{\nu} \bar{\nu}^T\right) \quad (11)$$

and

$$B = \begin{pmatrix} \frac{\partial m_i}{\partial \rho_j} \end{pmatrix}$$

Finally, having computed K, the matrices π and Z are updated by

$$\left. \begin{aligned} \pi &= (I - KB)M \\ Z &= (I - KB) \left(\Theta Z_k + \Gamma P_k \right) \Phi^T \end{aligned} \right\} \quad (12)$$

where all matrices without subscripts are understood to have subscript k+1. The accuracy of the estimation process is obtained from the π matrix.

Measurement constraint. - The angle between the line of sight to the sun and the CSM is determined by

$$\zeta = \cos^{-1} \left(\frac{-\bar{u}_{SL} \bar{\rho}}{\|\bar{\rho}\|} \right)$$

where \bar{u}_{SL} is a unit vector in the direction of the sun. The critical angle ζ^* is

$$\zeta^* = 5^\circ + 25^\circ \left[1 - e^{-0.0154(\|\bar{\rho}\| - 40)} \right]$$

where $\|\bar{\rho}\|$ is given in nautical miles.

The criteria which must be met for an optical sighting to be made are as follows:

- (1) If $\|\bar{\rho}\| < 40$ nautical miles, make a measurement only if $\zeta > 5^\circ$.
- (2) If $\|\bar{\rho}\| \geq 40$ nautical miles, make a measurement only if $\zeta > \zeta^*$.

REFERENCES

1. Kalman, R. E.; Englar, T. S.; and Bucy, R. S.: Fundamental Study of Adaptive Control Systems. ASD-TR-61-27, Vol. I. Flight Control Laboratory, ASD, Air Force Systems Command, 1962.
2. Struble, Raimond A.: Nonlinear Differential Equations. McGraw-Hill Book Co., Inc., 1962.

"The aeronautical and space activities of the United States shall be conducted so as to contribute . . . to the expansion of human knowledge of phenomena in the atmosphere and space. The Administration shall provide for the widest practicable and appropriate dissemination of information concerning its activities and the results thereof."

—NATIONAL AERONAUTICS AND SPACE ACT OF 1958

NASA SCIENTIFIC AND TECHNICAL PUBLICATIONS

TECHNICAL REPORTS: Scientific and technical information considered important, complete, and a lasting contribution to existing knowledge.

TECHNICAL NOTES: Information less broad in scope but nevertheless of importance as a contribution to existing knowledge.

TECHNICAL MEMORANDUMS: Information receiving limited distribution because of preliminary data, security classification, or other reasons.

CONTRACTOR REPORTS: Scientific and technical information generated under a NASA contract or grant and considered an important contribution to existing knowledge.

TECHNICAL TRANSLATIONS: Information published in a foreign language considered to merit NASA distribution in English.

SPECIAL PUBLICATIONS: Information derived from or of value to NASA activities. Publications include conference proceedings, monographs, data compilations, handbooks, sourcebooks, and special bibliographies.

TECHNOLOGY UTILIZATION PUBLICATIONS: Information on technology used by NASA that may be of particular interest in commercial and other non-aerospace applications. Publications include Tech Briefs, Technology Utilization Reports and Notes, and Technology Surveys.

Details on the availability of these publications may be obtained from:

SCIENTIFIC AND TECHNICAL INFORMATION DIVISION
NATIONAL AERONAUTICS AND SPACE ADMINISTRATION

Washington, D.C. 20546